The *Drosophila* insulin-degrading enzyme restricts growth by modulating the PI3K pathway in a cell-autonomous manner

Diego Galagovsky[a], Maximiliano J. Katz[a,b,*], Julieta M. Acevedo[a,b,*], Eleonora Sorianello[a,b], Alvaro Glavic[c], and Pablo Wappner[a,b,d]

[a]Instituto Leloir, Buenos Aires C1405BWE, Argentina; [b]National Scientific and Technical Research Council, Buenos Aires C1033AAJ, Argentina; [c]Centro FONDAP de Regulación del Genoma, Facultad de Ciencias, Universidad de Chile, Santiago 7800024, Chile; [d]Departamento de Fisiología, Biología Molecular y Celular, Facultad de Ciencias Exactas y Naturales, Universidad de Buenos Aires, Buenos Aires C1053ABJ, Argentina

ABSTRACT **Mammalian insulin-degrading enzyme (IDE) cleaves insulin, among other peptidic substrates, but its function in insulin signaling is elusive. We use the *Drosophila* system to define the function of IDE in the regulation of growth and metabolism. We find that either loss or gain of function of *Drosophila* IDE (dIDE) can restrict growth in a cell-autonomous manner by affecting both cell size and cell number. dIDE can modulate *Drosophila* insulin-like peptide 2 levels, thereby restricting activation of the phosphatidylinositol-3-phosphate kinase pathway and promoting activation of *Drosophila* forkhead box, subgroup O transcription factor. Larvae reared in high sucrose exhibit delayed developmental timing due to insulin resistance. We find that dIDE loss of function exacerbates this phenotype and that mutants display increased levels of circulating sugar, along with augmented expression of a lipid biosynthesis marker. We propose that dIDE is a modulator of insulin signaling and that its loss of function favors insulin resistance, a hallmark of diabetes mellitus type II.**

Monitoring Editor
Marianne Bronner
California Institute of Technology

Received: Apr 24, 2013
Revised: Dec 24, 2013
Accepted: Jan 3, 2014

INTRODUCTION

In animals, proper balance of energy uptake, storage, and utilization relies on coordinated communication between different tissues and organs to adjust metabolism according to organism needs. This is achieved through paracrine and endocrine signals that act at the cellular level to activate signaling pathways that mediate cell and organism adaptation. Central among these pathways is the phosphatidylinositol-3-phosphate kinase (PI3K) pathway, an evolutionarily conserved signaling cascade that adjusts metabolism according to nutrient availability (Britton *et al.*, 2002; Teleman, 2010). In mammals, glucose levels and metabolism are fine-tuned by insulin, which is secreted by pancreatic β-cells and delivered through the bloodstream to target tissues. Insulin binds its receptor on the plasma membrane of target tissues, activating the PI3K signaling pathway, which increases glucose uptake, storage, and utilization (Leto and Saltiel, 2012).

The insulin signaling pathway is highly conserved between mammals and *Drosophila* (Bohni *et al.*, 1999; Edgar, 2006). In *Drosophila*, eight insulin-like peptides (dILPs 1–8), homologous to mammalian insulin, bind a single receptor, activating the canonical PI3K pathway (Brogiolo *et al.*, 2001; Gronke *et al.*, 2010; Colombani *et al.*, 2012; Garelli *et al.*, 2012). In the fruit fly the insulin signaling pathway not only regulates metabolism through a unique insulin receptor, but also controls tissue growth in a similar way as insulin-like growth factors (IGFs) and IGF receptors do in mammals (Edgar, 2006). For this reason, the insulin cascade is known as the insulin/insulin-like signaling (IIS) pathway. dILP and IIS signaling is central for coupling growth and developmental programs with the nutritional status of the organism (Edgar, 2006).

In recent years, significant information has been gained regarding the control of dILP transcription and release (Ikeya *et al.*, 2002;

This article was published online ahead of print in MBoC in Press (http://www.molbiolcell.org/cgi/doi/10.1091/mbc.E13-04-0213) on January 15, 2014.

*These authors contributed equally to this work.

Address correspondence to: Pablo Wappner (pwappner@leloir.org.ar).

Abbreviations used: dIDE, *Drosophila* insulin-degrading enzyme; dILP2, *Drosophila* insulin-like peptide 2; DMII, diabetes mellitus type II; FOXO, *Drosophila* forkhead box, subgroup O transcription factor; IDE, insulin-degrading enzyme; PI3K, phosphatidylinositol-3-phosphate kinase; PTEN, *Drosophila* phosphatase and tensin homologue on chromosome 10.

Supplemental Material can be found at:
http://www.molbiolcell.org/content/suppl/2014/01/14/mbc.E13-04-0213.DC1.html

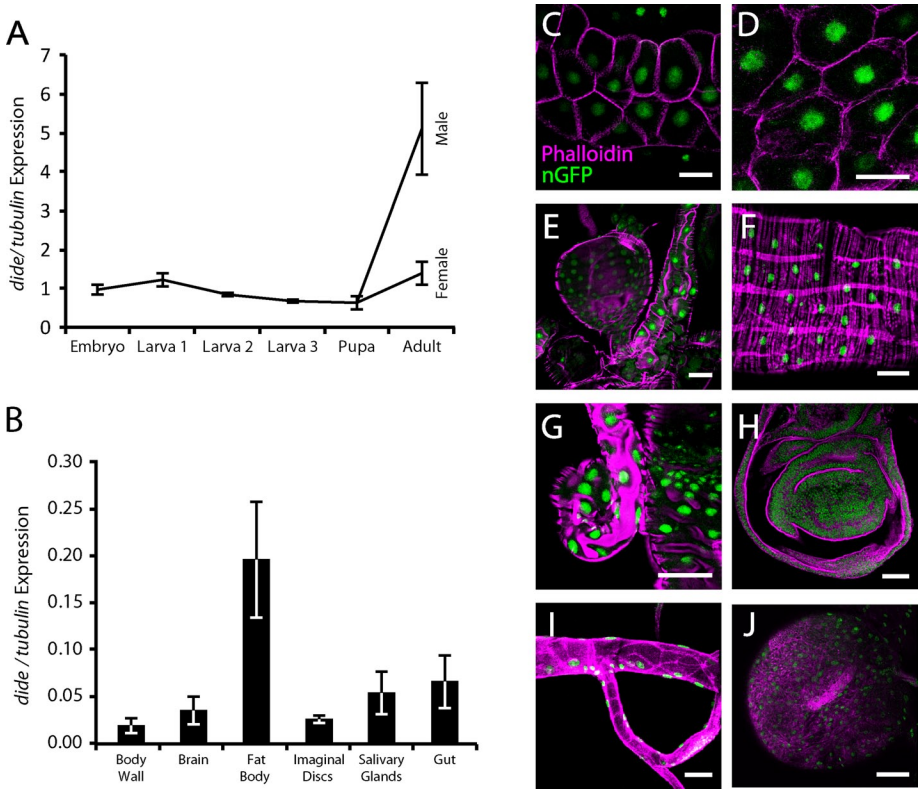

FIGURE 1: dIDE gene expression pattern. (A) Temporal variation of the expression of *dide* throughout the life cycle, as determined by qRT-PCR. Error bars represent SD (three independent experiments). (B) Expression of *dide* in third-instar larval organs. mRNA levels were determined by qRT-PCR. Error bars represent SD (three independent experiments). (C–J) Expression of *dide* in third-instar larval organs, as revealed by expression of a nuclear GFP reporter under the control of the *dide* promoter; representative organs. (C) Salivary glands, (D) fat body, (E) anterior gut and proventriculus, (F) midgut, (G) hindgut, (H) wing imaginal disc, (I) tracheae, and (J) brain. Bars, 50 µm.

Geminard *et al.*, 2009; Gronke *et al.*, 2010), but little is known about how dILP activity is terminated. This is an important aspect of IIS pathway regulation since, to attain a correct physiological outcome, not only is it important to have tight regulation of the initiation of the response, but it is also critical to shut down the cascade when it is no longer needed (Duckworth *et al.*, 1998). Evidence for insulin degradation as a plausible mechanism for IIS down-regulation emerged with the description of the insulin-degrading enzyme (IDE), a zinc metalloprotease with the capacity to cleave a wide array of small peptides, with insulin being the substrate with highest affinity (Duckworth *et al.*, 1998). Although the structure of human IDE has been resolved and its biochemical mechanism of action described in some detail, the physiological relevance of its insulin-degrading activity is unclear (Shen *et al.*, 2006; Im *et al.*, 2007).

The *Drosophila melanogaster* insulin-degrading enzyme (dIDE) displays 44% amino acid identity with human IDE (Shen *et al.*, 2006) and is capable of cleaving mammalian insulin in vitro (Garcia *et al.*, 1988; Duckworth *et al.*, 1989; Kuo *et al.*, 1991). Its overexpression provokes phenotypes that are presumably related to insulin deficiency (Tsuda *et al.*, 2010). The variety of genetic tools available in the fruit fly, the increasing knowledge on IIS pathway regulation, and the occurrence of structural and functional similarities with mammalian systems (Teleman, 2010) provide an opportunity to use this model organism to define the involvement of IDE in PI3K signaling and associated pathologies.

In the present study we use the *Drosophila* system to explore the relationship between dIDE and the IIS pathway. Through a genetic approach, we analyze the ability of dIDE to regulate *Drosophila* insulin-like peptide 2 (dILP2) levels and thereby modulate metabolism and growth in a normal or a high-sugar diet. We propose that dIDE is a negative regulator of the PI3K pathway and that dIDE loss of function contributes to insulin resistance.

RESULTS

dIDE is expressed ubiquitously

To begin investigating the function of dIDE, we analyzed the temporal and spatial expression pattern of its transcript. We extracted total RNA at different stages of the fruit fly life cycle and analyzed dIDE transcript levels by real-time PCR. We observed that dIDE mRNA levels are maximal in adult males, although dIDE expression can be detected throughout the life cycle (Figure 1A). Next we compared the expression of the transcript in different larval tissues, finding that the highest expression occurs in the fat body, with significant expression in other tissues as well (Figure 1B). In publicly available databases on high-throughput transcriptomic analyses, those variations of dIDE expression in the life cycle and between organs have not been observed (Graveley *et al.*, 2011; Marygold *et al.*, 2013). To complete the analysis of dIDE transcriptional profile, we isolated a genomic region encompassing 2.9 kb upstream of the dIDE translation initiation site, including the dIDE putative promoter, and generated a *dide*–green fluorescent protein (GFP) reporter line. As depicted in Figure 1, C–J, the reporter was strongly expressed in salivary glands (Figure 1C), fat body (Figure 1D), gut (Figure 1, E–G), imaginal disc (Figure 1H), tracheae (Figure 1I), and brain (Figure 1J). Taken together, these results suggest that dIDE is expressed in all *Drosophila* organs and cell types throughout the life cycle.

dIDE can modulate dILP levels

Because insulin is the most prominent substrate of mammalian IDE, we sought to analyze whether dIDE is capable of cleaving dILPs. Available anti-dILP antibodies are not sensitive enough to detect endogenous dILPs in Western blots, but one antibody can recognize overexpressed levels of this peptide (Figure 2A). We therefore performed an experiment in which dIDE and dILP2 were coexpressed ubiquitously and analyzed the levels of dILP2. dIDE was expressed throughout development in a UAS-dIDE transgenic line controlled by an actin-Gal4 driver in combination with the expression of dILP2 under direct control of a heat shock promoter. dILP2 was induced by exposing third-instar larvae to a 15-min heat shock, 4 h after which, whole-body homogenates were prepared for Western blot analysis. As shown in Figure 2, A and B, dILP2 levels were significantly reduced in larvae that overexpressed dIDE. These results suggest that the metalloprotease dIDE can cleave dILP2.

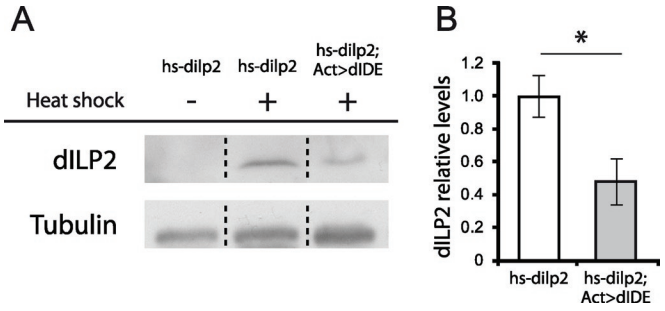

FIGURE 2: dIDE expression reduces dILP2 levels. (A) Anti-dILP2 Western blot of whole third- instar larval extracts prepared from individuals overexpressing dILP2 and coexpressing or not dIDE. Expression of dIDE provokes reduction of dILP2 levels. (B) Quantification of the Western blot. Error bars represent SEM (*$p < 0.05$; Student's *t* test, $n = 5$).

dIDE provokes growth reduction in a cell-autonomous manner

Given that dIDE is capable of reducing dILP2 levels, we sought to determine whether expression of this metalloprotease affects growth. Initially, we expressed dIDE ubiquitously through an actin-Gal4 driver and observed 12.3% reduction of pupal volume in comparison to control individuals (Figure 3A). One possibility is that dIDE cleaves dILPs in the hemolymph, thereby limiting their access to target tissues. If this were the case, the effect of dIDE manipulation would be systemic rather than cell autonomous. We investigated this issue in wing discs. The adult wing is a bilayer of cells, so growth defects in the wing disc dorsal compartment give rise to a smaller dorsal wing layer that ultimately generates wings that are curved upward (Raisin *et al.*, 2003). This was exactly what we observed after expressing dIDE in this disc territory: the wings were curved upward (Figure 3, B and C), indicating that dIDE can restrict growth in a cell-autonomous manner. To further analyze and quantify this effect, we expressed dIDE at the wing disc posterior compartment by using an engrailed-Gal4 driver (en-Gal4); we observed 19.1% reduction of region D of the wing at the posterior compartment (Birdsall *et al.*, 2000), suggesting again that the effect of dIDE is cell autonomous (Figure 3, D–F). Because insulin signaling is known to regulate organ growth by controlling both cell number and cell size, we quantified the contribution to growth reduction of each of these two parameters. To this end, we determined cell density at the posterior compartment of the wing by counting the hairs in a fixed area. The quantification revealed that IDE overexpression increases cell density by 11.2%, and therefore the cells are on average 11.2% smaller than those of control wings (Figure 3G). Because cell size reduction accounts only partially for posterior compartment reduction (19.1%), we inferred that the latter originates from a combination of reduced cell size and reduced cell number. These conclusions were further confirmed by counting directly the cells after overexpression of dIDE under control of a *patched*-Gal4 driver in region C of the wing (Figure 3D). Also in this case, reduction of the area occurred specifically in the wing territory that overexpressed the enzyme, and this reduction resulted from a combination of decreased cell size and decreased cell number (Supplemental Figure S1).

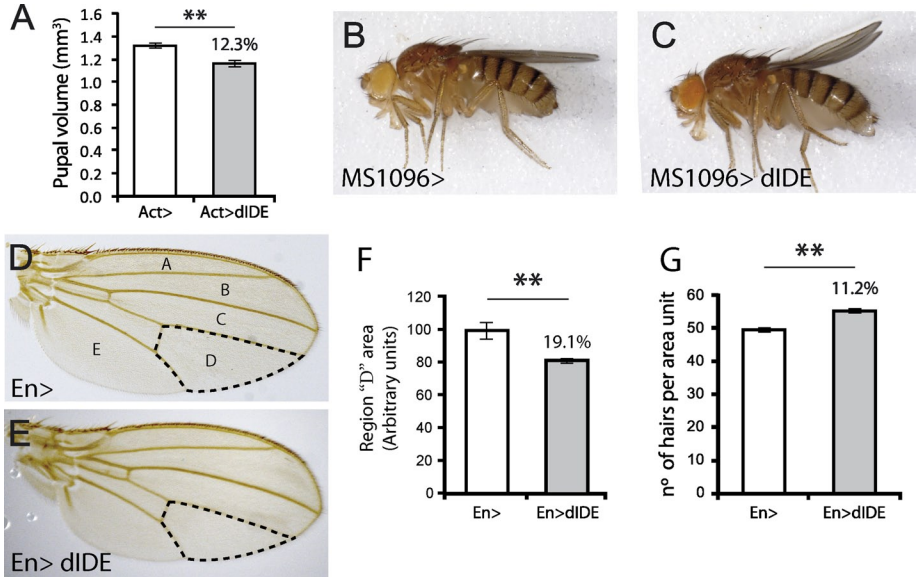

FIGURE 3: dIDE provokes growth reduction in a cell-autonomous manner. (A) Pupae from individuals that express transgenic dIDE ubiquitously are significantly smaller than those of control siblings, as determined by their pupal volume (see *Materials and Methods*). Error bars represent SEM (**$p < 0.001$; Student's *t* test; $n \geq 30$ in three independent experiments). (B, C) Expression of dIDE in the dorsal compartment of the wing imaginal disc generates upwardly curved wings, indicating reduction of growth of this compartment. (D, E) Expression of dIDE at the posterior compartment of the disc provokes a reduction of the posterior half of the wing; this was estimated by measuring the area of the wing region D (indicated by the broken line in D, E). (F) Quantification of wing areas marked in D and E. Error bars represent SEM (**$p < 0.001$; Student's *t* test; $n \geq 20$ in three independent experiments). (G) Wing hair density at the posterior compartment of the wing. Following expression of dIDE, hair density increased, indicating that cell size was reduced. Cell size reduction accounts only partially for reduction of the area of the wing posterior compartment; compare delta values in F (19.1%) and G (11.2%). The remaining reduction of the area is due to decreased number of cells in the compartment. Error bars represent SEM (**$p < 0.001$; Student's *t* test; $n \geq 20$ in three independent experiments).

dIDE-dependent growth reduction is mediated by the PI3K pathway in a cell-autonomous manner

Given that dILPs activate the PI3K pathway upon binding the insulin receptor (InR), we sought to investigate whether regulation of this pathway mediates the effect of dIDE. *Drosophila* phosphatase and tensin homologue on chromosome 10 (PTEN) is a phosphatidylinositol (3,4,5)-triphosphate phosphatase that negatively regulates PI3K signaling downstream of the InR (Goberdhan *et al.*, 1999; Huang *et al.*, 1999), so it is expected that PTEN reduction of function will antagonize the effect of dIDE. Indeed, as depicted in Figure 4, A–C and E, loss of one dose of PTEN largely suppresses dIDE-dependent growth impairment, supporting the notion that dIDEs exerts its effect by modulating PI3K pathway activation.

The PI3K pathway signals in part through *Drosophila* forkhead box, subgroup O transcription factor (FOXO). Activation of the cascade leads to phosphorylation and nuclear exclusion of FOXO, resulting in reduced FOXO-dependent transcription (Junger *et al.*, 2003; Puig *et al.*, 2003). To investigate whether dILP-dependent reduction of growth is mediated in part by FOXO,

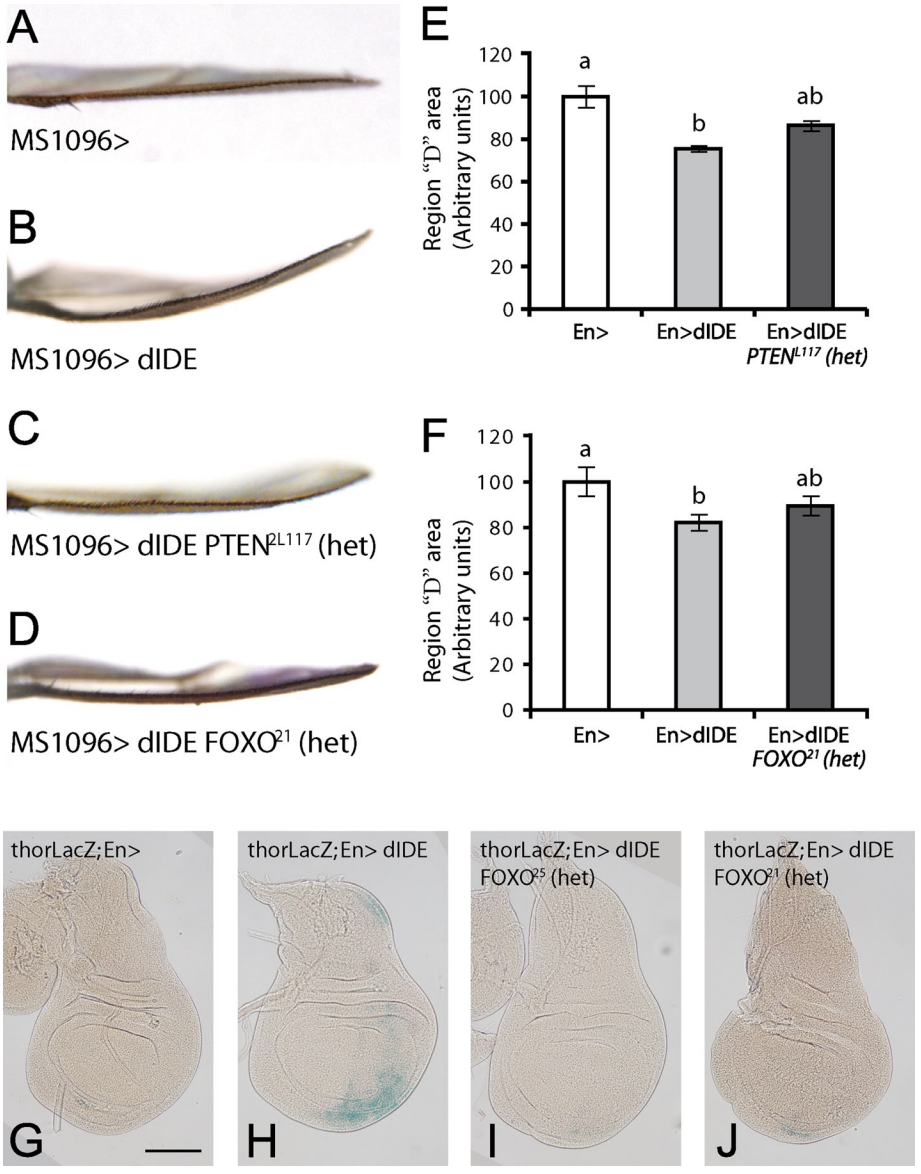

FIGURE 4: Reduction of growth upon dIDE expression is mediated by the PI3K pathway. (A–D) The wing curvature provoked by the expression dIDE at the dorsal compartment of the imaginal disc (A, B) is partially suppressed in flies lacking one dose of PTEN (C) or FOXO (D). (E, F) Reduction of the area of the posterior compartment provoked by the expression of dIDE under control of an *en*-Gal4 driver (assessed by determination of the wing region D) is partially reverted in individuals lacking one dose of PTEN (E) or FOXO (F). These results (A–F) indicate that the PI3K pathway mediates dIDE-dependent growth reduction through the regulation of FOXO. Error bars represent SEM ($p < 0.05$; one-way analysis of variance (ANOVA) with Tukey post hoc test; means with a letter in common are not significantly different; $n \geq 20$ in three independent experiments). (G, H) The FOXO target gene *thor* is induced at the posterior compartment of the wing imaginal disc upon expression of dIDE in the same compartment, suggesting that dIDE-dependent inactivation of the PI3K pathway and activation of FOXO is cell autonomous. In *foxo*^{25} (I) or *foxo*^{21} (J) heterozygous mutant larvae, dIDE-dependent *thor* transcription is reduced, confirming that FOXO mediates *thor-LacZ* induction in this setting. Bar, 100 μm.

we took a genetic approach similar to that described for PTEN. We observed that FOXO reduction of function antagonized the effect of dIDE, as the wing curvature observed upon expression of dIDE in the dorsal compartment was partially suppressed in FOXO-heterozygous individuals (Figure 4, A, B, and D), and similarly, the reduction of the wing posterior compartment observed upon *en*-Gal4 driven expression of dIDE was also suppressed in FOXO heterozygotes (Figure 4F). To confirm that dIDE can increase FOXO-dependent transcription, we examined the induction of the FOXO target gene *thor* (Teleman *et al.*, 2005) by using a *thor*-LacZ enhancer trap. As depicted in Figure 4, G and H, β-galactosidase expression was detected only at the posterior wing disc compartment of en-Gal4/UAS-dIDE individuals, confirming that dIDE indeed induces FOXO-dependent transcription and that the effect of dIDE is cell autonomous. Consistent with the experiments described earlier, expression of *thor*-LacZ was largely suppressed in larvae that were heterozygous for FOXO (Figure 4, I and J). Taken together, these results suggest that dIDE-dependent growth reduction is mediated by a cell-autonomous mechanism that involves the negative regulation of the PI3K pathway and consequent activation of the transcription factor FOXO.

dIDE accumulates in the cytoplasm and plasma membrane of the cells in which it is expressed

The cell-autonomous effect of dIDE suggested that the enzyme is not secreted freely to the hemolymph but instead exerts its effect locally in the cell in which it is expressed. To analyze this, we generated a transgenic line expressing a dIDE:GFP fusion protein, which was initially induced at the wing imaginal disc under control of a *ptc*-Gal4 driver. dIDE:GFP did not diffuse away from the row of *ptc*-positive cells (Figure 5A). Instead, part of the fusion protein accumulated at the plasma membrane, and no protein could be detected at the lumen of the imaginal disc between the columnar epithelium and the peripodial membrane (Figure 5, B and C). The expression of dIDE:GFP in the *patched* expression pattern provokes reduction of the distance between veins III and IV, which is even more pronounced than the reduction elicited by the expression of the untagged dIDE (Figure 5, D–G). This indicates that dIDE:GFP is biologically active, suggesting that subcellular localization of the GFP fusion protein recapitulates the localization of endogenous dIDE. *ptc*-Gal4 drives transgene expression also in the salivary gland, so we studied subcellular localization of dIDE:GFP in this organ. In this case too, the fusion protein appeared to be retained in the cytosol and accumulated in the plasma membrane, whereas no protein appeared to be secreted to the extracellular milieu (Supplemental Figure S2, A–F). Remarkably, the size of the salivary gland expressing dIDE:GFP was autonomously reduced (Supplemental Figure S2, G and H), confirming again that the effect of dIDE is cell autonomous. Taken together, the foregoing experiments suggest that dIDE is retained in the cytoplasm and plasma membrane of the cell in

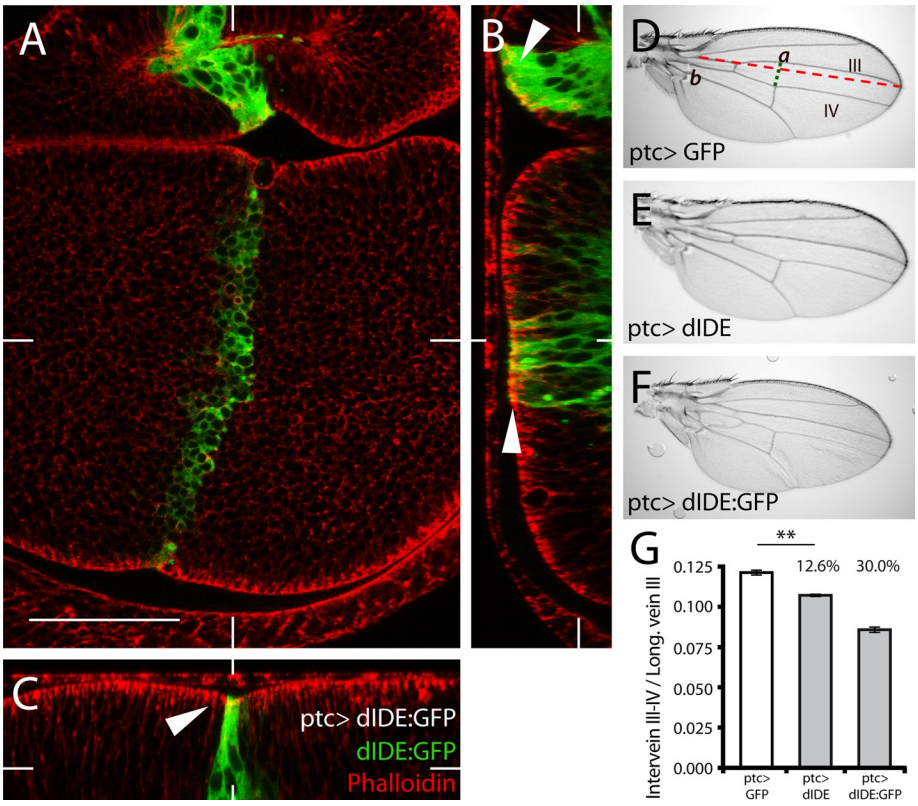

FIGURE 5: dIDE localizes in the cytoplasm and plasma membrane of wing imaginal disc cells. Expression of a dIDE:GFP fusion protein was induced in the wing imaginal disc through a *ptc*-Gal4 driver. (A) The fusion protein can be detected only in the narrow stripe of cells (two to four cells) that expresses *patched*, without any indication that the protein can move away into neighboring cells. (B) Longitudinal and (C) transverse *z*-sections of the wing disc showing that the fusion protein accumulates in the cytoplasm and plasma membrane (arrowheads) of *ptc*-expressing cells; scale bar, 50 μm. (D–F) The expression of dIDE (E) or dIDE:GFP (F) under control of the *ptc*-Gal4 driver reduces the distance between veins III and IV (shown in D) as compared with control wings expressing GFP alone (D). (G) Quantification of the effect of dIDE or dIDE:GFP expression on the reduction of the distance between veins III and IV. The effect of dIDE:GFP (30% reduction) is stronger than that of dIDE alone (12.6% reduction). The distance between veins III and IV is indicated as *a* (green line) in D. The distance *a* was normalized to the length of vein III, indicated as *b* (red line; $^{**}p < 0.001$; one-way ANOVA with Tukey post hoc test; $n \geq 20$ in three independent experiments).

which it is expressed, explaining its cell-autonomous effect on growth regulation and modulation of the PI3K pathway.

Down-regulation of dIDE provokes reduction of tissue growth and sensitizes developmental timing and metabolism to high-sucrose diets

Next we sought to study the effect of dIDE loss of function on growth and metabolism. We analyzed in detail a dIDE-null mutant line generated by gene targeting (Tsuda *et al.*, 2010) and found that pupal volume of these mutants is significantly reduced in comparison to wild-type siblings (Figure 6A). dIDE RNA interference (RNAi) is efficient in mediating reduction of dIDE transcript levels (Supplemental Figure S3), so it was used to analyze whether the growth reduction observed in the dIDE mutants is cell autonomous. Indeed, this was the case, as expression of the RNAi in the wing disc dorsal compartment provoked a clear reduction of compartment size (Figure 6, B and C, and Supplemental Figure S4), which resulted in adult wings that were curved upward (Figure 6D and E). Similarly, expression of dIDE RNAi at the posterior compartment of the wing disc provoked a clear (13.9%) reduction of the area of the posterior compartment of the wing in comparison to control flies (Figure 6F). Taken together, the results indicate that dIDE loss of function provokes growth reduction in a cell-autonomous manner. As a next step, we investigated whether reduced activation of the PI3K pathway accounts for growth reduction also in this setting. Following an approach similar to the one utilized earlier, we expressed dIDE RNAi in the wing disc posterior compartment of larvae that were heterozygous for PTEN or FOXO mutant alleles. Area reduction of the posterior wing compartment was strongly suppressed in both PTEN (3.2%) and FOXO (3.9%) heterozygotes (Figure 6, F and G), suggesting that reduction of PI3K signaling accounts for growth impairment upon dIDE silencing. To get further evidence that FOXO mediates this growth reduction, we examined whether transcript levels of the FOXO target gene *thor* increase upon expression of dIDE RNAi. Silencing of dIDE in the fat body provoked strong up-regulation of *thor* transcription, and this up-regulation was completely suppressed in PTEN-heterozygous larvae (Supplemental Figure S5). Taken together, these results indicate that dIDE silencing provokes activation of the transcription factor FOXO through the inhibition of the PI3K pathway.

Given that dIDE can negatively regulate dILP availability and growth (Figure 2) and that this effect is mediated by the PI3K pathway (Figure 4), the reduction of growth observed upon dIDE knockdown seems paradoxical at first glance. However, it was recently shown that *Drosophila* larvae reared in a high-sucrose diet, albeit displaying augmented levels of circulating dILPs, exhibit reduced growth and delayed developmental timing (Musselman *et al.*, 2011; Pasco and Leopold, 2012). Physiological characterization of these larvae revealed that growth impairment was due to a phenomenon known as insulin resistance (Musselman *et al.*, 2011; Pasco and Leopold, 2012). We therefore investigated whether dIDE loss of function enhances insulin resistance in *Drosophila* larvae exposed to a high-sucrose diet.

We raised wild-type individuals and larvae homozygous for the $dIDE^{KO}$ null allele either in regular food (0.2 M sucrose) or in a high-sucrose culture medium (1 M sucrose). As depicted in Figure 6H, under regular feeding conditions, wild-type and IDE^{KO} larvae developed almost at the same rate. As previously reported (Musselman *et al.*, 2011; Pasco and Leopold, 2012), in high-sucrose medium wild-type larvae exhibited a conspicuous developmental delay, pupariating 3 d later than in normal culture medium. Of interest, the delay provoked by the high-sugar diet was enhanced in $dIDE^{KO}$ larvae, which pupariated >1 d later than wild-type individuals (Figure 6H). Similar results were obtained when reduction of dIDE levels were attained by ubiquitous expression of dIDE RNAi (Supplemental Figure S6).

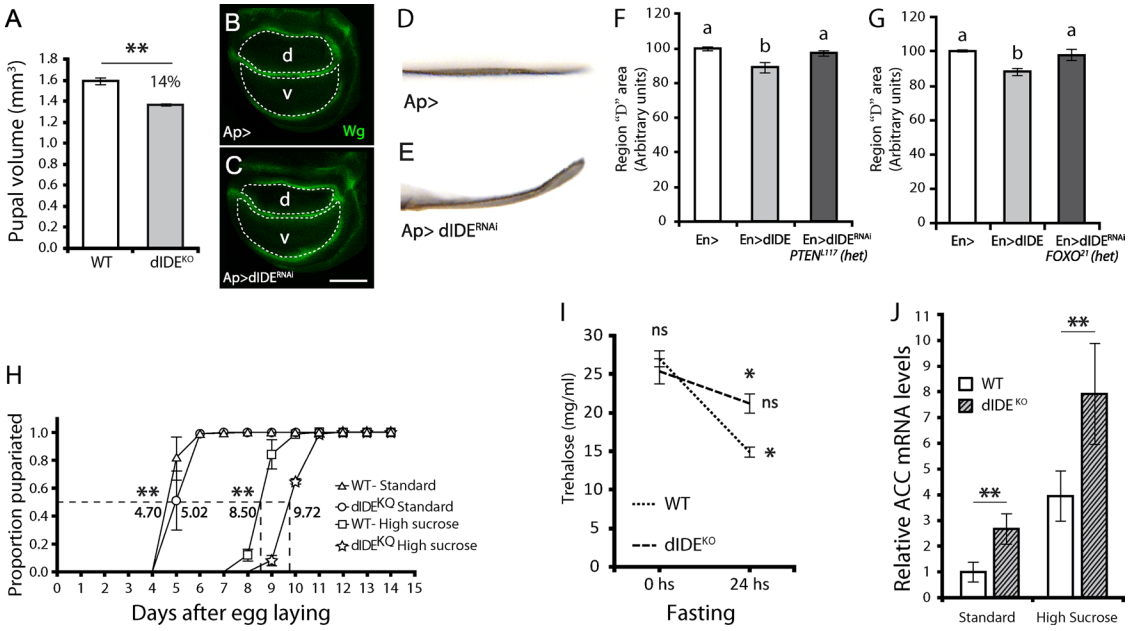

FIGURE 6: dIDE loss of function provokes reduction of growth and sensitization to a high-sugar diet. (A) dIDE^{KO} pupae are significantly smaller than those of control (WT) siblings, as assessed by calculating their pupal volume (see *Materials and Methods*). Error bars represent SEM (**$p < 0.001$; Student's t test; $n \geq 30$ in three independent experiments). (B, C) The dorsal compartment of the wing imaginal disc is autonomously reduced upon dIDE RNAi expression. Disc compartments can be visualized by the expression of Wingless (Wg, green); d, disc dorsal compartment; v, disc ventral compartment. Bar, 100 µm. (D, E) dIDE^{RNAi}-dependent autonomous growth reduction of the dorsal compartment resulted in wings curved upward. (F, G) dIDE^{RNAi} expression at the posterior compartment of the wing disc provoked autonomous reduction of this compartment, as assessed by determination of the area of region D. Expression of RNAi in PTEN (F) or FOXO (G) heterozygous mutants caused strong suppression of growth impairment. Error bars represent SEM ($p < 0.05$; one way ANOVA with Tukey post hoc test; means with a letter in common are not significantly different; $n \geq 20$ in three independent experiments). (H) dIDE^{KO} and control larvae pupariate almost at the same time in standard culture medium. In a high-sugar culture medium, significant delay of pupariation of wild-type individuals occurred; this delay was increased in dIDE^{KO} larvae. Error bars represent SD (**$p < 0.001$; two-way ANOVA with Duncan post hoc test; $n = 60$ in six independent experiments). (I) In WT adult flies, trehalose levels in hemolymph dropped significantly after 24-h starvation; in dIDE^{KO} individuals subjected to starvation, trehalose levels remained similar to those of well-fed animals. Error bars represent SEM (ns, non significant; *$p < 0.05$; two-way ANOVA with Tukey post hoc test; $n = 5$). (J) dIDE^{KO} flies display augmented levels of the acetyl CoA carboxylase (ACC) transcript, used as an indicator of TAG metabolism. In high-sugar medium, ACC expression increased significantly in wild-type larvae, but ACC transcript levels in dIDE^{KO} individuals were even higher. Error bars represent SEM (**$p < 0.001$; two-way ANOVA with Tukey post hoc test; $n = 3$).

In mammals, insulin resistance provokes hyperglycemia in fasting conditions, derived in part from reduced capacity of the tissues to incorporate glucose, resulting in higher-than-normal circulating sugar levels. To test whether dIDE^{KO} individuals display this metabolic phenotype, we subjected wild-type and dIDE^{KO} adult flies to 24-h starvation, after which we measured circulating levels of the disaccharide trehalose, the main circulating sugar in insects. As depicted in Figure 6I, in wild-type flies trehalose levels dropped sharply after 24-h starvation, whereas in dIDE^{KO} flies, trehalose levels remained close to those observed before starvation. These results suggest that dIDE is necessary for adjusting the levels of circulating sugar levels in response to variations of the feeding conditions.

Obesity is another feature associated with insulin resistance, which originates at least in part from higher-than-normal levels of circulating triacylglycerol (TAG) and increased lipid storage. TAG levels are known to be regulated the PI3K pathway in *Drosophila* (Xu *et al.*, 2012). It was reported that increased lipid levels correlate with augmented expression of the acetyl CoA carboxylase (ACC) gene transcript (Pasco and Leopold, 2012), the enzyme that catalyses the first step in fatty acid biosynthesis. We analyzed transcription of ACC in dIDE^{KO} and wild-type larvae reared in either regular medium or a high-sugar diet. We found that ACC transcription was strongly upregulated in IDE^{KO} flies in both regular and high-sugar food (Figure 6J), suggesting that dIDE knockdown affects lipid metabolism. Taken together, the foregoing results suggest that dIDE loss of function favors the manifestation of several phenotypes that are related to insulin resistance.

DISCUSSION

In this work we showed that dIDE has the capacity to modulate dILP2 levels, regulate the PI3K pathway, and affect growth. The growth phenotypes observed upon dIDE manipulation depend at least in part on the transcription factor FOXO, one of the main effectors of the PI3K pathway. Because dIDE-null mutants are homozygous viable to adulthood, dIDE is probably not a core regulator of the PI3K pathway but instead a modulator of this cascade that contributes to fine-tuning fly growth and metabolism. We showed that both dIDE gain and loss of function bring about diminished growth, results that, at first glance, seem paradoxical. Nevertheless, diminished signaling in conditions of increased insulin has been reported

and is known as insulin resistance, a hallmark of human diabetes mellitus type II (DMII; Zimmet *et al.*, 2001). In a DMII *Drosophila* model, larvae fed with a high-sugar diet display higher-than-normal levels of circulating dILP2, along with reduced PI3K signaling in target tissues (Musselman *et al.*, 2011; Pasco and Leopold, 2012).

The mechanisms of the genesis and progression of DMII are unclear. Although obesity, high-sugar diets, and fat-rich diets are well-established predisposition factors for the disease (Zimmet *et al.*, 2001; Venables and Jeukendrup, 2009), genetic risk factors have also been proposed (Stumvoll *et al.*, 2008; Ridderstrale and Groop, 2009). It is noteworthy that association between IDE loss-of-function and DMII has been reported, as human populations with mutations in the IDE locus display increased incidence of this disease (Karamohamed *et al.*, 2003; Rudovich *et al.*, 2009). In keeping with this observation, the GK rat, an animal model that recapitulates most of the features of human DMII (Goto *et al.*, 1976), was found to carry loss-of-function mutations in the IDE locus (Fakhrai-Rad *et al.*, 2000; Farris *et al.*, 2004). Experimental evidence for a role of IDE in the etiology of DMII came shortly afterward with the generation of IDE-knockout mice, which display hyperinsulinemia and glucose intolerance (Farris *et al.*, 2003; Abdul-Hay *et al.*, 2011). Even though the mechanisms linking IDE to the genesis of DMII are elusive, a simple explanation would be that reduced degradation of insulin leads to increased insulinemia, which in turn provokes reduced insulin sensitivity due to increased receptor internalization. In this simplistic model, IDE is predicted to operate in the bloodstream, mediating insulin clearance from circulation. If this model is correct, IDE should be secreted from the cell and mediate insulin degradation extracellularly (i.e., in the bloodstream), behaving in a nonautonomous manner.

Although several studies revealed that IDE can be secreted to the extracellular milieu (Goldfine *et al.*, 1984; Seta and Roth, 1997; Vekrellis *et al.*, 2000; Bulloj *et al.*, 2010), other works reported the occurrence of the enzyme at other locations, such as the plasma membrane, endosomes, peroxisomes, mitochondria, and cytosol (Hamel *et al.*, 1991; Authier *et al.*, 1994; Morita *et al.*, 2000; Leissring *et al.*, 2004). In rat liver parenchymal cells the early endosome is a major site of degradation of insulin, although IDE was found to be cytosolic and thus is apparently not involved in endosomal degradation in this tissue (Pease *et al.*, 1985; Backer *et al.*, 1990; Doherty *et al.*, 1990; Authier *et al.*, 1994).

In the present study, we found that IDE is in part associated with the plasma membrane, without any evidence of its being secreted. We provided clear evidence that its effect on growth regulation is cell autonomous, and so it is its capacity to modulate activation of the PI3K pathway. Thus, based on our genetic evidence, an attractive possibility is that dIDE is associated to plasma membrane domains that are in close proximity to insulin receptors, and so after binding of the ligand, dIDE is endocyted together with the receptor–ligand complex. Once in early endosomes, dIDE cleaves the ligand, contributing to recycling the receptor to the plasma membrane.

Of interest, it was suggested for other receptor tyrosine kinases that cleavage of the ligand at the early endosome is important for recycling the receptor to the plasma membrane (Sorkin and Von Zastrow, 2002). So, if *Drosophila* IDE does indeed exert its function at early endosomes, knockdown of dIDE is expected to cause reduction of dILP proteolysis in this compartment, leading to impairment of recycling of insulin receptors to the membrane, ultimately provoking insulin resistance. In this scenario, overexpression of dIDE may increase dILP proteolysis at the plasma membrane before ligand binding to the receptor, thereby reducing PI3K signaling. Detailed biochemical and cellular studies are required to define the precise subcellular location of dIDE and particularly the functional relevance of its possible role in early endosomes.

MATERIALS AND METHODS

Fly stocks

For the generation of UAS-dIDE lines we amplified the *dide* open reading frame by PCR from the EST RE17458 (DGRC). For generation of the *dide* nGFP expression reporter we cloned a 2-kb fragment upstream of the translation initiation site with the primers 5′-GGGGTACCCCTTGGGTTTTATAAGCGTGCCAATCG-3′ and 5′-GAAGATCTTCAATACATGGCAATCGGTTCCAC-3′, which include sites for *Kpn*I and *Bgl*II, in a pStinger (Barolo *et al.*, 2000) nGFP vector. For the UAS-dIDE:GFP transgenic line we cloned the dIDE gene by removing the stop codon by PCR using the primers 5′-GACGAATTCATGTATCTTACGTGCAGAAAATCG-3′ and 5′-CGGGGTACCGTAAGCTTGCTGCGTGCTCCCTTCG-3′ (including sites for *Eco*RI and *Kpn*I restriction enzymes, respectively) into a pEGFP-N1 plasmid and then subcloned the fusion protein construct into a pUAST-attB plasmid (Bischof *et al.*, 2007). Transgenic lines were generated by embryo germline transformation (Spradling and Rubin, 1982).

We used the following stocks from the Bloomington *Drosophila* Stock Center (Indiana University, Bloomington, IN): *En-Gal4* (#6356), *MS1096* (#8696), *Ap-Gal4* (#3041), *Act-Gal4* (#3954, #4414), *ptc-Gal4* (#2017), and $thor^{1}$ (#9558). The following stocks were from the Vienna *Drosophila* RNAi Center: UAS-$dIDE^{RNAi}$ (#15957 and #15958) and UAS-Dcr2 (#60009). The following stocks were obtained from different colleagues: $PTEN^{2L117}$ (Oldham *et al.*, 2000), $FOXO^{21}$ and $FOXO^{25}$ (Junger *et al.*, 2003), hs-dilp2 (Rulifson *et al.*, 2002), and IDE^{KO} (Tsuda *et al.*, 2010). Controls for the experiments with IDE^{KO} mutants were performed in the y,w background line.

Anti-dILP2 Western blots

First-instar larvae overexpressing or not dIDE were sorted and placed in groups of 60 individuals/vial. First, larvae were exposed to a 15-min heat shock at 37°C and then placed at 25°C for 4 h. Larvae were then recovered, rinsed in phosphate-buffered saline (PBS), and homogenized in lysis buffer (50 mM Tris, pH 8, 150 mM NaCl, 1 mM ethylene glycol tetraacetic acid, 1% NP-40, Sigma Protease Inhibitor Cocktail). After centrifugation, samples were loaded in 10% SDS–PAGE gels, run, and transferred to an Immobilon-P^{SQ} membrane (Millipore, Billerica, MA). Membranes were incubated with 1:1000 anti-dilp2 antibody (gift from Hugo Stocker, ETHZ, Zürich, Switzerland), revealed with Amersham ECL Prime (GE Healthcare, Pittsburgh, PA), and scanned. Bands were quantified using ImageJ software (National Institutes of Health, Bethesda, MD).

Immunostaining and X-Gal staining

For immunostaining, larvae were dissected in PBS and fixed in PBS/Triton 0.1% (PBST) and formaldehyde 4% for 20 min at room temperature. Samples were washed with PBST and blocked with PBST bovine serum albumin 5%, followed by incubation with a primary antibody overnight at 4°C, washed, and incubated 4 h at room temperature with secondary antibodies conjugated to fluorophores. Phalloidin (1:200; Sigma, St. Louis, MO) was added during the last 30 min of secondary antibody incubation. Samples were then washed and mounted in PBST glycerol 80%. Antibodies used in this study were anti-GFP (1:1000, A-11122; Invitrogen, Carlsbad, CA) and anti-Wingless (1:1000, 4D4; Developmental Studies Hybridoma Bank, Iowa City, IA). Images were captured in a Carl Zeiss LSM510 Meta Confocal Microscope.

For X-Gal staining, larvae were dissected in PBS and fixed 10 min in a 16.67 mM KH_2PO_4/K_2HPO_4 (pH 6.8), 75 mM KCl, 25 mM NaCl,

3.33 mM $MgCl_2$, 5% glutaraldehyde buffer at room temperature. Samples were then washed with PBST and incubated overnight with the staining solution (5 µM $K_4Fe(CN)_6$, 5 µM $K_3Fe(CN)_6$, 0.2%X-Gal) at room temperature. Samples were then washed and mounted for observation and photographed using an Olympus BX60 microscope equipped with an Olympus DP71 digital camera.

Quantitative real-time PCR

The following primers were used for quantitative real-time PCR (qRT-PCR): for dIDE, 5′-CAACGCCGCCACCTATCC-3′ and 5′-AGAGTTTACCGCATTGATTTCCC-3′; for dILP2, 5′-ATCCCGTGATTCCACACAAG-3′ and 5′-GCGGTTCCGATATCGAGTTA-3′; for ACC, 5′-GCTTGCGTGATCCCTCGTT-3′ and 5′-GATATGGGTATGCGACCAGAGAT-3′; and for Rpl29 to normalize the quantifications. qRT-PCR was performed using a Mx3005P QPCR System (Stratagene, La Jolla, CA).

Wing measurements

First-instar larvae of the different genotypes were sorted and placed in groups of 60 individuals/vial and allowed to develop to adulthood. The 2- to 4-d-old adults were collected and conserved in 70% ethanol until analysis. The right wings of female individuals were removed and mounted in a lactic acid:ethanol (1:1) mixture. Photographs of the wings were taken with an Olympus MVX10 stereomicroscope with an Olympus DP71 digital camera. Quantification of the areas was performed with ImageJ.

Developmental timing and pupal size

First-instar larvae of the different genotypes were sorted against fluorescent balancer chromosomes and placed in groups of 60 individuals/vial and raised at 25°C. Developmental timing was assessed by counting the pupae in each vial every day at noon. Results were plotted, and curves were approximated to a Gompetz model using Infostat Statistical Software (Universidad Nacional de Córdoba, Córdoba, Argentina). The α, β, and γ parameters were calculated, and the time of 50% pupariation was determined for each repeat.

For determining pupal size, pupae were photographed at 10× magnification under an Olympus MVX10 stereomicroscope with an Olympus DP71 camera and measured using ImageJ. Pupal volume was estimated by adjusting it to the volume of a pill with hemispheric ends ($V = \pi D^2(3L - D)/12$, where D is the width and L is the length of the pupa). Standard and high-sugar culture media were prepared as previously described (Pasco and Leopold, 2012).

Trehalose determinations

The 2- to 4-d-old adults of each genotype were placed in vials in groups of 25 and maintained for 24 h in standard feeding conditions, after which they were transferred for fasting to 3.5-cm-diameter Petri dishes lined with a piece of Whatman No. 1 paper wet in PBS. Hemolymph was extracted from groups of 14 females by puncturing the thorax with a 0.15-gauge entomological needle and placed on a makeshift cage on the top of a 1.5-ml Eppendorf tube with a 22-nm nylon mesh. The tubes were centrifuged at 2600 × g for 5 min at 4°C. Hemolymph was diluted 1:20 in water and heated to 95°C for 5 min. Two microliters of sample were mixed with Fisher Hexokinase Reagent (Fisher Scientific, Pittsburgh, PA), and, after 15-min reaction, absorbance at 340 nm was recorded using a Nanodrop 1000 apparatus (Thermo Scientific, Wilmington, DE).

Statistical analysis

Infostat Statistical Software and Excel (Microsoft, New York, NY) were used for statistical analysis where appropriate.

ACKNOWLEDGMENTS

We thank Hugo Stocker for the dILP2 antibody, Alejandro Rabossi for technical assistance with hemolymph extractions, the many laboratories that generated transgenic and mutant stocks used in this study, the Vienna *Drosophila* RNAi Center, the Bloomington *Drosophila* Stock Center, and members of Pablo Wappner's laboratory for insightful comments and discussion. This work was funded by Wellcome Trust Grant WT087675MA and Agencia de Promoción Científica y Tecnológica Grant PICT 2011 No. 0090.

REFERENCES

Abdul-Hay SO, Kang D, McBride M, Li L, Zhao J, Leissring MA (2011). Deletion of insulin-degrading enzyme elicits antipodal, age-dependent effects on glucose and insulin tolerance. PLoS One 6, e20818.

Authier F, Rachubinski RA, Posner BI, Bergeron JJ (1994). Endosomal proteolysis of insulin by an acidic thiol metalloprotease unrelated to insulin degrading enzyme. J Biol Chem 269, 3010–3016.

Backer JM, Kahn CR, White MF (1990). The dissociation and degradation of internalized insulin occur in the endosomes of rat hepatoma cells. J Biol Chem 265, 14828–14835.

Barolo S, Carver LA, Posakony JW (2000). GFP and beta-galactosidase transformation vectors for promoter/enhancer analysis in *Drosophila*. BioTechniques 29, 726, 728, 730, 732.

Birdsall K, Zimmerman E, Teeter K, Gibson G (2000). Genetic variation for the positioning of wing veins in *Drosophila melanogaster*. Evol Dev 2, 16–24.

Bischof J, Maeda RK, Hediger M, Karch F, Basler K (2007). An optimized transgenesis system for *Drosophila* using germ-line-specific phiC31 integrases. Proc Natl Acad Sci USA 104, 3312–3317.

Bohni R, Riesgo-Escovar J, Oldham S, Brogiolo W, Stocker H, Andruss BF, Beckingham K, Hafen E (1999). Autonomous control of cell and organ size by CHICO, a *Drosophila* homolog of vertebrate IRS1–4. Cell 97, 865–875.

Britton JS, Lockwood WK, Li L, Cohen SM, Edgar BA (2002). *Drosophila*'s insulin/PI3-kinase pathway coordinates cellular metabolism with nutritional conditions. Dev Cell 2, 239–249.

Brogiolo W, Stocker H, Ikeya T, Rintelen F, Fernandez R, Hafen E (2001). An evolutionarily conserved function of the *Drosophila* insulin receptor and insulin-like peptides in growth control. Curr Biol 11, 213–221.

Bulloj A, Leal MC, Xu H, Castano EM, Morelli L (2010). Insulin-degrading enzyme sorting in exosomes: a secretory pathway for a key brain amyloid-beta degrading protease. J Alzheimers Dis 19, 79–95.

Colombani J, Andersen DS, Leopold P (2012). Secreted peptide Dilp8 coordinates *Drosophila* tissue growth with developmental timing. Science 336, 582–585.

Doherty JJ 2nd, Kay DG, Lai WH, Posner BI, Bergeron JJ (1990). Selective degradation of insulin within rat liver endosomes. J Cell Biol 110, 35–42.

Duckworth WC, Bennett RG, Hamel FG (1998). Insulin degradation: progress and potential. Endocrine Rev 19, 608–624.

Duckworth WC, Garcia JV, Liepnieks JJ, Hamel FG, Hermodson MA, Frank BH, Rosner MR (1989). *Drosophila* insulin degrading enzyme and rat skeletal muscle insulin protease cleave insulin at similar sites. Biochemistry 28, 2471–2477.

Edgar BA (2006). How flies get their size: genetics meets physiology. Nat Rev Genet 7, 907–916.

Fakhrai-Rad H, Nikoshkov A, Kamel A, Fernstrom M, Zierath JR, Norgren S, Luthman H, Galli J (2000). Insulin-degrading enzyme identified as a candidate diabetes susceptibility gene in GK rats. Hum Mol Genet 9, 2149–2158.

Farris W, Mansourian S, Chang Y, Lindsley L, Eckman EA, Frosch MP, Eckman CB, Tanzi RE, Selkoe DJ, Guenette S (2003). Insulin-degrading enzyme regulates the levels of insulin, amyloid beta-protein, and the beta-amyloid precursor protein intracellular domain in vivo. Proc Natl Acad Sci USA 100, 4162–4167.

Farris W, Mansourian S, Leissring MA, Eckman EA, Bertram L, Eckman CB, Tanzi RE, Selkoe DJ (2004). Partial loss-of-function mutations in insulin-degrading enzyme that induce diabetes also impair degradation of amyloid beta-protein. Am J Pathol 164, 1425–1434.

Garcia JV, Fenton BW, Rosner MR (1988). Isolation and characterization of an insulin-degrading enzyme from *Drosophila melanogaster*. Biochemistry 27, 4237–4244.

Garelli A, Gontijo AM, Miguela V, Caparros E, Dominguez M (2012). Imaginal discs secrete insulin-like peptide 8 to mediate plasticity of growth and maturation. Science 336, 579–582.
Geminard C, Rulifson EJ, Leopold P (2009). Remote control of insulin secretion by fat cells in *Drosophila*. Cell Metab 10, 199–207.
Goberdhan DC, Paricio N, Goodman EC, Mlodzik M, Wilson C (1999). *Drosophila* tumor suppressor PTEN controls cell size and number by antagonizing the Chico/PI3-kinase signaling pathway. Genes Dev 13, 3244–3258.
Goldfine ID, Williams JA, Bailey AC, Wong KY, Iwamoto Y, Yokono K, Baba S, Roth RA (1984). Degradation of insulin by isolated mouse pancreatic acini. Evidence for cell surface protease activity. Diabetes 33, 64–72.
Goto Y, Kakizaki M, Masaki N (1976). Production of spontaneous diabetic rats by repetition of selective breeding. Tohoku J Exp Med 119, 85–90.
Graveley BR *et al*. (2011). The *D. melanogaster* transcriptome: modENCODE RNA-Seq data for dissected tissues. Available at: http://flybase.org/reports/FBrf0213503.html (accessed 13 April 2011).
Gronke S, Clarke DF, Broughton S, Andrews TD, Partridge L (2010). Molecular evolution and functional characterization of *Drosophila* insulin-like peptides. PLoS Genet 6, e1000857.
Hamel FG, Mahoney MJ, Duckworth WC (1991). Degradation of intraendosomal insulin by insulin-degrading enzyme without acidification. Diabetes 40, 436–443.
Huang H, Potter CJ, Tao W, Li DM, Brogiolo W, Hafen E, Sun H, Xu T (1999). PTEN affects cell size, cell proliferation and apoptosis during *Drosophila* eye development. Development 126, 5365–5372.
Ikeya T, Galic M, Belawat P, Nairz K, Hafen E (2002). Nutrient-dependent expression of insulin-like peptides from neuroendocrine cells in the CNS contributes to growth regulation in *Drosophila*. Curr Biol 12, 1293–1300.
Im H *et al*. (2007). Structure of substrate-free human insulin-degrading enzyme (IDE) and biophysical analysis of ATP-induced conformational switch of IDE. J Biol Chem 282, 25453–25463.
Junger MA, Rintelen F, Stocker H, Wasserman JD, Vegh M, Radimerski T, Greenberg ME, Hafen E (2003). The *Drosophila* forkhead transcription factor FOXO mediates the reduction in cell number associated with reduced insulin signaling. J Biol 2, 20.
Karamohamed S *et al*. (2003). Polymorphisms in the insulin-degrading enzyme gene are associated with type 2 diabetes in men from the NHLBI Framingham Heart Study. Diabetes 52, 1562–1567.
Kuo WL, Gehm BD, Rosner MR (1991). Regulation of insulin degradation: expression of an evolutionarily conserved insulin-degrading enzyme increases degradation via an intracellular pathway. Mol Endocrinol 5, 1467–1476.
Leissring MA, Farris W, Wu X, Christodoulou DC, Haigis MC, Guarente L, Selkoe DJ (2004). Alternative translation initiation generates a novel isoform of insulin-degrading enzyme targeted to mitochondria. Biochem J 383, 439–446.
Leto D, Saltiel AR (2012). Regulation of glucose transport by insulin: traffic control of GLUT4. Nat Rev Mol Cell Biol 13, 383–396.
Marygold SJ, Leyland PC, Seal RL, Goodman JL, Thurmond J, Strelets VB, Wilson RJ (2013). FlyBase: improvements to the bibliography. Nucleic Acids Res 41, D751–D757.
Morita M, Kurochkin IV, Motojima K, Goto S, Takano T, Okamura S, Sato R, Yokota S, Imanaka T (2000). Insulin-degrading enzyme exists inside of rat liver peroxisomes and degrades oxidized proteins. Cell Struct Funct 25, 309–315.
Musselman LP, Fink JL, Narzinski K, Ramachandran PV, Hathiramani SS, Cagan RL, Baranski TJ (2011). A high-sugar diet produces obesity and insulin resistance in wild-type *Drosophila*. Dis Model Mech 4, 842–849.
Oldham S, Montagne J, Radimerski T, Thomas G, Hafen E (2000). Genetic and biochemical characterization of dTOR, the *Drosophila* homolog of the target of rapamycin. Genes Dev 14, 2689–2694.
Pasco MY, Leopold P (2012). High sugar-induced insulin resistance in *Drosophila* relies on the lipocalin Neural Lazarillo. PLoS One 7, e36583.
Pease RJ, Smith GD, Peters TJ (1985). Degradation of endocytosed insulin in rat liver is mediated by low-density vesicles. Biochem J 228, 137–146.
Puig O, Marr MT, Ruhf ML, Tjian R (2003). Control of cell number by *Drosophila* FOXO: downstream and feedback regulation of the insulin receptor pathway. Genes Dev 17, 2006–2020.
Raisin S, Pantalacci S, Breittmayer JP, Leopold P (2003). A new genetic locus controlling growth and proliferation in *Drosophila melanogaster*. Genetics 164, 1015–1025.
Ridderstrale M, Groop L (2009). Genetic dissection of type 2 diabetes. Mol Cell Endocrinol 297, 10–17.
Rudovich N, Pivovarova O, Fisher E, Fischer-Rosinsky A, Spranger J, Mohlig M, Schulze MB, Boeing H, Pfeiffer AF (2009). Polymorphisms within insulin-degrading enzyme (IDE) gene determine insulin metabolism and risk of type 2 diabetes. J Mol Med (Berl) 87, 1145–1151.
Rulifson EJ, Kim SK, Nusse R (2002). Ablation of insulin-producing neurons in flies: growth and diabetic phenotypes. Science 296, 1118–1120.
Seta KA, Roth RA (1997). Overexpression of insulin degrading enzyme: cellular localization and effects on insulin signaling. Biochem Biophys Res Commun 231, 167–171.
Shen Y, Joachimiak A, Rosner MR, Tang WJ (2006). Structures of human insulin-degrading enzyme reveal a new substrate recognition mechanism. Nature 443, 870–874.
Sorkin A, Von Zastrow M (2002). Signal transduction and endocytosis: close encounters of many kinds. Nat Rev Mol Cell Biol 3, 600–614.
Spradling AC, Rubin GM (1982). Transposition of cloned P elements into *Drosophila* germ line chromosomes. Science 218, 341–347.
Stumvoll M, Goldstein BJ, van Haeften TW (2008). Type 2 diabetes: pathogenesis and treatment. Lancet 371, 2153–2156.
Teleman AA (2010). Molecular mechanisms of metabolic regulation by insulin in *Drosophila*. Biochem J 425, 13–26.
Teleman AA, Chen YW, Cohen SM (2005). 4E-BP functions as a metabolic brake used under stress conditions but not during normal growth. Genes Dev 19, 1844–1848.
Tsuda M, Kobayashi T, Matsuo T, Aigaki T (2010). Insulin-degrading enzyme antagonizes insulin-dependent tissue growth and Abeta-induced neurotoxicity in *Drosophila*. FEBS Lett 584, 2916–2920.
Vekrellis K, Ye Z, Qiu WQ, Walsh D, Hartley D, Chesneau V, Rosner MR, Selkoe DJ (2000). Neurons regulate extracellular levels of amyloid beta-protein via proteolysis by insulin-degrading enzyme. J Neurosci 20, 1657–1665.
Venables MC, Jeukendrup AE (2009). Physical inactivity and obesity: links with insulin resistance and type 2 diabetes mellitus. Diabetes Metab Res Rev 25 (Suppl 1), S18–S23.
Xu X, Gopalacharyulu P, Seppanen-Laakso T, Ruskeepaa AL, Aye CC, Carson BP, Mora S, Oresic M, Teleman AA (2012). Insulin signaling regulates fatty acid catabolism at the level of CoA activation. PLoS Genet 8, e1002478.
Zimmet P, Alberti KG, Shaw J (2001). Global and societal implications of the diabetes epidemic. Nature 414, 782–787.